Taylor & Francis
Taylor & Francis Group

Preparative Biochemistry & Biotechnology

ISSN: 1082-6068 (Print) 1532-2297 (Online) Journal homepage: www.tandfonline.com/journals/lpbb20

Optimization of chitosan-PEG-geranium oil nanoparticles and in-vitro studies on pancreatic ductal adenocarcinoma

Keerthi V. , Aparna Naguraj T. , Manjunathan Jagadeesan , Pasiyappazham Ramasamy , Ambiga Somasundaram , Chandramohan Govindasamy , Khalid M. Almutairi , Krishna Prakash Arunachalam & Meenambiga Setti Sudharsan

To cite this article: Keerthi V. , Aparna Naguraj T. , Manjunathan Jagadeesan , Pasiyappazham Ramasamy , Ambiga Somasundaram , Chandramohan Govindasamy , Khalid M. Almutairi , Krishna Prakash Arunachalam & Meenambiga Setti Sudharsan (16 Apr 2026): Optimization of chitosan-PEG-geranium oil nanoparticles and in-vitro studies on pancreatic ductal adenocarcinoma, Preparative Biochemistry & Biotechnology, DOI: 10.1080/10826068.2026.2654610

To link to this article: https://doi.org/10.1080/10826068.2026.2654610

Published online: 16 Apr 2026.

PREPARATIVE BIOCHEMISTRY & BIOTECHNOLOGY
https://doi.org/10.1080/10826068.2026.2654610

Optimization of chitosan-PEG-geranium oil nanoparticles and in-vitro studies on pancreatic ductal adenocarcinoma

Keerthi V.[a], Aparna Naguraj T.[a], Manjunathan Jagadeesan[b], Pasiyappazham Ramasamy[c], Ambiga Somasundaram[d], Chandramohan Govindasamy[e], Khalid M. Almutairi[e], Krishna Prakash Arunachalam[f] and Meenambiga Setti Sudharsan[a]

[a]Department of Bioengineering, School of Engineering, Vels Institute of Science Technology and Advanced Studies (VISTAS), Chennai, India; [b]Department of Biotechnology, School of life Sciences, Vels Institute of Science Technology and Advanced Studies (VISTAS), Chennai, India; [c]Marine Biopolymer Research Lab, Centre for Marine and Aquatic Research (CMAR), Saveetha Dental College & Hospitals, Saveetha Institute of Medical and Technical Sciences (SIMATS), Saveetha University, Chennai, India; [d]Department of Physiology, Saveetha Dental College & Hospitals, Saveetha Institute of Medical and Technical Sciences (SIMATS), Saveetha University, Chennai, India; [e]Department of Community Health Sciences, College of Applied Medical Sciences, King Saud University, Riyadh, Saudi Arabia; [f]Departamento de Ciencias de la Construcción, Facultad de Ciencias de la Construcción Ordenamiento Territorial, Universidad Tecnológica Metropolitana, Santiago, Chile

ABSTRACT

Pancreatic ductal adenocarcinoma (PDAC) is a highly aggressive cancer with limited therapeutic options and is expected to become the second leading cause of cancer-related deaths by 2030. Geraniol, a naturally occurring monoterpenoid found in essential oils, has demonstrated anticancer activity but its clinical use is restricted by poor solubility and low bioavailability. In this study, geraniol was encapsulated within chitosan–polyethylene glycol (CS–PEG) nanocarriers using an ionic interaction method to enhance its therapeutic efficacy. Formulation parameters were optimized using a statistical design approach to evaluate the influence of polymer and surfactant concentrations on encapsulation efficiency. The optimized formulation showed strong model validity ($p < 0.005$; $F = 6.89$) and achieved an encapsulation efficiency of 93.87%. Physicochemical characterization confirmed an amorphous structure with an average particle size below 250 nm. *In vitro* cytotoxicity and apoptosis assessments using MTT and AO/PI assays on pancreatic cancer cell lines revealed enhanced, dose-dependent anticancer activity. The CS–PEG–geraniol nanocarriers demonstrated significantly greater efficacy at 100 µg/mL compared to free geraniol. Overall, the findings suggest that CS–PEG nanocarriers represent a promising and biocompatible delivery platform for improving geraniol-based therapy against PDAC.

KEYWORDS

Chitosan/PEG nanoparticle; controlled release of therapeutic drug; geraniol; health; pancreatic ductal adenocarcinoma (PDAC); response surface methodology (RSM)

Introduction

One of the most aggressive and deadly types of cancer, Pancreatic Ductal Adenocarcinoma (PDAC) is frequently linked to poor clinical results and a high death rate. This is primarily attributed to its silent progression—nonspecific and asymptomatic early-stage presentation—which results in most cases being diagnosed only at an advanced or metastatic stage. By the time of diagnosis, PDAC shows extensive systemic distribution because of its aggressive nature and delayed discovery. Pancreatic cancer was the sixth most common disease globally in 2018, accounting for about 4.5% of all cancer-related fatalities.[1] As a result of the disease's dismal prognosis, the situation became even more concerning in 2020, when the number of deaths (466,000) was almost equal to the total number of new cases (496,000).[2] Since a large percentage of patients (80–85%) receive their diagnosis after the cancer has spread and there are few available treatments, the five-year overall survival rate is still a pitiful 10%.

The KRASG12D mutation is one of the main genetic changes causing PDAC; it encourages tumor growth, resistance to apoptosis, and a poor response to treatment.[3] While the KRAS oncogene presents a promising target for intervention, its direct inhibition has proven challenging. In this context, natural compounds like geraniol have gained attention for their anticancer potential. It has been demonstrated that the naturally occurring monoterpene geraniol inhibits cell proliferation and induces apoptosis in various malignancies.[4] However, its therapeutic utility is limited due to poor solubility, low bioavailability, and rapid metabolic degradation. To address these limitations, this study utilizes nanoencapsulation techniques to enhance the stability and bioavailability of geraniol derivatives, thereby improving their anticancer efficacy. Nano formulations were developed

CONTACT Pasiyappazham Ramasamy ramkanth281@gmail.com Marine Biopolymer Research Lab, Centre for Marine and Aquatic Research (CMAR), Saveetha Dental College & Hospitals, Saveetha Institute of Medical and Technical Sciences (SIMATS), Saveetha University, Chennai, Tamil Nadu, 600077, India; Meenambiga Setti Sudharsan meenambiga.se@velsuniv.ac.in Department of Bioengineering, School of Engineering, Vels Institute of Science Technology and Advanced Studies (VISTAS), Pallavaram, Chennai, Tamil Nadu, 600 117, India.

using ionic gelation method, which allows for uniform and dense polymerization and encapsulation of Chitosan and STPP with geranium oil and optimized drug delivery against the target. The resulting nanoparticles were characterized to evaluate their physical and functional attributes. Dynamic Light Scattering (DLS) was employed to determine particle size distribution and polydispersity index, while zeta potential analysis provided insights into surface charge and colloidal stability. Crystallinity and structural properties were examined using X-ray Diffraction (XRD). Morphological evaluation was conducted through Scanning Electron Microscopy (SEM), and cellular internalization was confirmed via fluorescence microscopic imaging. Furthermore, cytotoxicity studies through cell viability assays and apoptosis assays by dual staining were carried out to assess the safety (only targeting cancer cells) and efficacy of the nanoformulated compounds in inducing cancer cell death without affecting the normal cells.

Materials and methods

Experimental design

The Chitosan/Polyethylene glycol-geranium oil nanoparticle (CS/PEG GONPs) was optimized based on a three-factor, three-level Box-Behnken Design (BBD). Independent variables (factors) that were being studied includes chitosan concentration (A), PEG concentration (B), and surfactant concentration (C). They were represented by the values +1, 0, and, −1 representing high, medium, and low levels, respectively (Table 1). The range was chosen as follows: chitosan concentration (0.2–2 mg/mL), PEG concentration (0.1–0.3%), and surfactant (1–5%) based on preliminary optimization studies and literature evidence.[5–7] Encapsulation efficiency (EE%) (Y_i) was applied as dependent variable (response). The interaction of independent variables and responses were assessed using the following quadratic mathematical model Eq. (1):

$$Y = b_0 - b_1X_1 - b_2X_2 + b_3X_3 - b_{12}X_1X_2 + b_{23}X_2X_3 + b_{13}X_1X_3 + b_{11}X_1^2 + b_{22}X_2^2 + \boldsymbol{b}_{33}X_3^2 \quad (1)$$

where X_i stands for the coded independent variables, b_i is the predicted regression coefficient for each factor, b_0 is the arithmetic mean response of 17 runs, and Y_i is the dependent variable.[8] Statistical analysis from formulation design was carried out using Stat-Ease 360 trial software. For RSM analysis, the software-generated experimental design matrix and related observations for the dependent variables are performed and entered.

Table 1. Variables employed in Box-Behnken design.

	Levels		
Independent variable/factor	−1	0	1
X_1: Chitosan concentration (mg/mL)	0.2	1.1	2
X_2: PEG concentration (%)	0.1	0.2	0.3
X_3: Surfactant concentration (%)	1	3	5
Dependent variable\response	Constraints		
Y_1: Encapsulation efficiency (%)	Maximize		

Preparation of geranium oil standard solution and calibration curve

Gernaium oil *(Pelargonium graveolens*; HiMedia Laboratories Pvt. Ltd., Mumbai, India) and absolute ethanol (100%; HiMedia Laboratories Pvt. Ltd., Mumbai, India) was employed to prepare the Geranium stock solution as they don't interfere with the Geranium oil absorbance. The stock solution was further diluted between 1% and 5%. The diluted solutions' absorbance in a UV/Vis Spectrophotometer at a wavelength of 310 nm was utilized to develop the standard calibration curve for oil.[9] Ethanol used for dissolving geranium oil was removed by continuous magnetic stirring until complete evaporation prior to nanoparticle collection.

Preparation of free and geranium-loaded CS/PEG nanoparticles

With minimal modifications in the method used by Melo et al.[10], chitosan/polyethylene glycol-geranium oil nanoparticles (CS-PEG GONPs) were formulated using the ionic gelation method. Stock solutions of chitosan (Medium MW extrapure, 150–500 m.pas, 90% DA, CAS Number 9012-76-4, Sigma Aldrich, USA) (2.0 mg/mL), polyethylene glycol (PEG) (Average MW = 380–420, CAS Number 25322-68-3, Merck, Germany) (0.3%), Tween 80 extrapure (CAS Number 9005-65-6, Sigma Aldrich, USA) (1%), and sodium tripolyphosphate (STPP) extrapure, 57–59% as P_2O_5 (MW = 367.86, CAS Number 7758-29-4, Sigma Aldrich, USA) (5%) were prepared according to the following instructions. Chitosan (2.0 mg/mL) was dissolved in 1% v/v aqueous solution of acetic acid with magnetic stirring at 100 rpm for 2 h at room temperature until a clear solution was achieved. The pH was thereafter raised to 5.0 with 0.5 M sodium hydroxide pellets extrapure AR, 98% (MW = 40, CAS Number 1310-73-2). Independently, PEG (0.3%), Tween 80 (1%), and STPP (5%) stock solutions were dissolved in distilled water with hand stirring. To prepare the CS/PEG nanoparticles, 1 mL of the PEG solution was slowly blended with the 20 mL of chitosan solution and magnetically stirred for 30 min with respective concentration (% and mg/mL) as given in the trials (RSM). Then, for another half hour, 80 µL of ge^{r}anium oil with 1 mL of 1% Tween was added and swirled. Finally, to ensure consistent gelation, 8 mL of respective concentration (%) of STPP was added as a crosslinking agent and the mixture was stirred for one hour at 25 °C.

Determination of encapsulation efficiency

In a cooling centrifuge, the homogenous solution containing CS-PEG GONPSs was made to spin for 30 min at 4 °C, 6000 rpm. A UV-Visible spectrophotometer set to 310 nm was used to measure the amount of geranium oil in the supernatant.[11] The ratio of the absorbance of the oil associated with the nanoparticles to the absorbance of the initial/total amount of oil supplied was used to calculate the encapsulation efficiency (EE).[12] This relationship was described by Eq. (2):

$$\mathrm{EE}(\%) = \frac{\text{Absorbance of initial oil} - \text{Absorbance of free oil}}{\text{Absorbance of initial oil}} * 100 \quad (2)$$

Statistical and check point analysis

To ensure the model fit, analysis of variance (ANOVA) and lack of fit were executed. The results were believed to be statistically significant when the p-value was below 0.05.[13] Response surfaces were plotted and thoroughly examined to figure out the effect of components (X1, X2, and X3) on the preparation of nanoparticles. In order to create nanoparticles with the highest EE, response surface analysis and a mathematical model were used to determine the CS-PEG GONPS theoretical ideal experimental settings. The experimental responses (Y1) were compared with the expected ones after the statistical models were verified in triplicates.

Characterization of nanoparticles

Polymeric nanoparticles that were produced were characterized by the second derivative peak search technique in an X-ray diffractometer with conventional 2θ geometry to evaluate the crystallinity pattern of the material. The Horiba SZ-100 Zetasizer was utilized to find out the size and polydispersity index (PDI) of the nanoparticles based on the Dynamic Light Scattering (DLS) method. Polystyrene cuvettes were filled with an aliquot (1 ml) of nanoparticle solutions, and the measurement was performed at 25 °C with a scattering angle of 90°.[14] For Scanning Electron Microscopy (SEM), liquid samples were dripped on carbon tape covered aluminum stubs, dried at 40 °C for 2 h, sputtered in the secondary electron mode (gold metallization), analyzed at 20 kW to determine the morphological properties.

Cell viability test

HPNE (Primary Human Pancreatic cell lines) and PANC-1 (Human Pancreatic cancer cell lines) were procured from ATCC. Cell lines were grown in high glucose Dulbecco's modified Eagle's medium (DMEM; EuroClone, Milan, Italy) supplemented with 10% fetal bovine serum ((FBS; Sigma-Aldrich, USA), 2 mM L-glutamine (2 mM; Merck, Germany)10, 100 U/mL penicillin, 1 mM sodium pyruvate (1 mM; Thermo Fisher Scientific, USA) and 100 mg streptomycin. Cell lines were preserved at 37 °C and 95% humidity and 5% CO_2. The anticancer potential of the sample was evaluated with the MTT (3-(4,5-dimethylthiazol-2-yl)-2,5 diphenyltetrazolium bromide, Sigma-Aldrich, USA) assay on HPNE and PANC-1 cell line. Seeded in 96-well microplates (1 x 10^4 cells/well), the cells were incubated at 37 °C for 48 h in a 5% CO_2 incubator until the cells were at 70–80% confluence. HPNE cell lines were treated with 100 µg/mL of GO and CS-PEG GONPSs and incubated for 72 h. PANC-1 cells were treated with different sample concentrations for 24 h and after 24 h, the morphological changes of untreated (control) and treated cells were analyzed and imaged with a digital inverted microscope (20X magnification). The HPNE and PANC-1 cells were then washed with phosphate-buffer saline (PBS, pH 7.4) and 20 µL of (MTT) solution (5 mg/mL in PBS) was added to each well. The plates were then made to stand at 37 °C in the dark for 4 h.[15] The formazan crystals were dissolved in 100 µL DMSO and the absorbance was read spectrometrically at 570 nm. Percentage of cell viability was calculated using the formula Eq. (3),

$$\text{Cell viability}(\%) = \frac{\text{Absorbance of sample}}{\text{Absorbance of control}} * 100 \quad (3)$$

Apoptosis fluorescent assay by dual AO/PI staining method

The PANC-1 (Human Pancreatic Cancer Cell line) (1×10^4) were added in 24-well plates and treated with GO and CS-PEG GONPSs separately for 24 h. The cells treated with Dulbecco's modified eagle medium (DMEM) and control drug was considered as control group. The treated cells were taken and washed with phosphate buffer saline. 5 µl of the fluorescent dye stain acridine orange (AO, Sigma-Aldrich, USA) (100 µg/mL) and 5 µl of propidium iodide (PI, Sigma-Aldrich, USA) (100 µg/mL) was added to it. Fluorescent dual staining assay with AO/PI was used in the study to identify the early and late apoptotic and necrotic cells. With dual staining method, the dead nucleated cells will be stained red and live cells appear green. The morphological changes were observed by a FLoid cell imaging fluorescent microscope.[16]

Results

To make sure that enough medication is delivered to the target area to generate a therapeutic effect, EE must be considered while developing drug delivery systems. By examining certain formulation and process factors in the early phases of development, these characteristics may be controlled. The prepared CS-PEG GONPSs was optimized in the current investigation using BBD. To assess the impact of three independent factors on a single dependent variable, a total of 17 runs with five center points were conducted.

Effect of independent variables on EE (Y1)

A complete Figure 1 full level factorial designs was shown in Table 2. The range of all encapsulation efficiency was 43.68% to 88.52%. To deduce the quantitative impacts of the factor components, an ANOVA analysis was conducted. Multiple regression analysis of data yielded a polynomial equation (quadratic model) for EE. If the p-value is less than 0.05 then model terms are significant. An antagonistic or inverse effect of the component on the response is indicated by a negative sign, while a positive number indicates a synergistic effect that supports optimization.[17] The actual Eq. (4) for dependent variable in terms of coded factors is presented below:

$$EE = 54.14 - 3.32A - 1.31B + 4.02C - 7.72AB + 8.82BC + 18.25A^2 + 7.07B^2 \quad (4)$$

The quadratic model was the proposed model to be significant for EE, given its R^2 value of 0.8428. The negative coefficients of A, B shows that the increase in Chitosan and

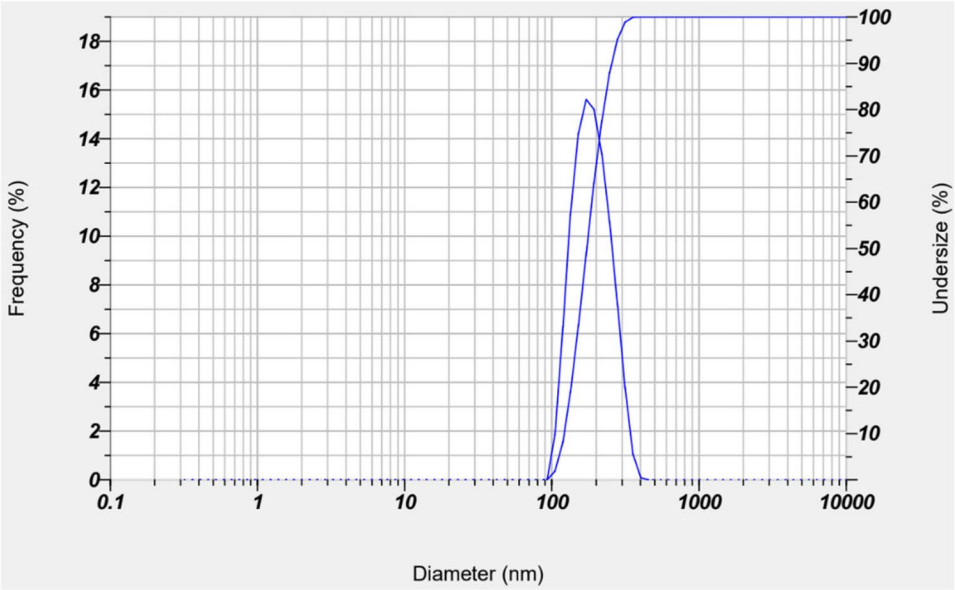

Figure 1. Particle size distribution of chitosan nanoparticles.

Table 2. Experimental runs for 3 full level factorial BBD design.

Chitosan concentration (mg/mL) (X_1)	PEG concentration (%) (X_2)	Surfactant concentration (%) (X_3)	EE (%) (Y_1)
1.1	0.2	3	54.71
1.1	0.2	3	55.51
1.1	0.3	5	75.02
2	0.1	3	88.25
2	0.2	1	64.64
1.1	0.2	3	43.68
2	0.2	5	65.73
1.1	0.3	1	46.99
0.2	0.3	3	82.29
1.1	0.1	1	68.83
1.1	0.1	5	61.58
0.2	0.2	5	88.52
1.1	0.2	3	54.75
1.1	0.2	3	54.44
0.2	0.2	1	78.26
2	0.3	3	71.77
0.2	0.1	3	67.91

PEG concentration may decrease the encapsulation efficiency. In addition, the negative coefficient of AB shows the increase of both Chitosan and PEG may result in the combined effect of decreasing the encapsulation efficiency than the individual effect. Furthermore, "Adequate precision" is frequently used to evaluate signal to noise ratio (predicted response related to its associated error) and this ratio of greater than four is usually desirable for navigating design space. With the signal to noise ratio value of 8.593, EE proved the high adequacy of the selected model. When the results were graphically represented for the tested response, the experimental data collected showed a high correlation with the expected data.

The non-significant lack of fit of the model ($p < 0.005$ at the 0.5% significance level) reveals that the data is fitting the suggested models. The F-value of the EE (quadratic) model of 6.89 shows that the model is significant. The coefficient of determination (R^2) from the ANOVA test was used to assess the influence of the independent variables on the dependent variable.[18] An R^2 value of 0.8428, or 84.28%, indicates that chitosan concentration, PEG concentration, and surfactant concentration collectively accounted for 84.28% of the variation in encapsulation efficiency. The remaining 15.72% is attributed to other factors not accounted by the model.

The coefficient of the model was significant in terms of F and p values, which were obtained from the ANOVA results (Table 3). The synergistic effect of A, B, C, AB, BC, A^2, and B^2 significantly influenced response Y1 (EE), with a p-value less than 0.05 for AB, BC, and A^2. Response surface methodology (RSM) was utilized to further define and examine the effect of independent variables on factors on responses. The parallel contour plots and RSG (Figure 2) that relate EE show that EE increases as all independent variable concentrations increase.

Optimized polymeric nanoparticle

The optimal experimental parameters to produce nanoscale particles with a high content of geranium essential oil were found by applying statistical tools and critically analyzing response surfaces. These were a concentration of chitosan of 0.2 mg/mL, a PEG concentration of 0.28 percent, and a surfactant concentration of 4.85 percent. Nanoparticles were formulated in triplicate under those conditions in order to test the model, and the outcomes were compared with the values that the model calculated, within a preferable error of less than 5%. Under these conditions, the predicted EE of the calculated model was 95.429%. The observed encapsulation efficiency (93.87%) was compatible with that of the predicted (95.429%) with a confidence interval of 95%. The estimated confidence interval (81.5567%–109.302%) is consistent with the experimental result for response Y1 (93.87%) of the improved formulation. Table 4 provided the predicted and actual encapsulation efficiency values for the improved nanoformulation.

Table 3. ANOVA results for independent variables obtained from RSM.

Source	Sum of squares	df	Mean square	F-value	P-value	
Model	2463.26	7	351.89	6.89	0.0050	Significant
A-Chitosan conc	88.38	1	88.38	1.73	0.2209	
B-PEG conc	13.78	1	13.78	0.2699	0.6160	
C-Surfactant conc	129.04	1	129.04	2.53	0.1464	
AB	238.08	1	238.08	4.66	0.0591	
BC	311.17	1	311.17	6.09	0.0357	
A^2	1406.22	1	1406.22	27.54	0.0005	
B^2	210.88	1	210.88	4.13	0.0727	
Residual	459.61	9	51.07			
Lack of fit	359.12	5	71.82	2.86	0.1654	Not significant
Pure error	100.49	4	25.12			
Cor Total	2922.87	16				

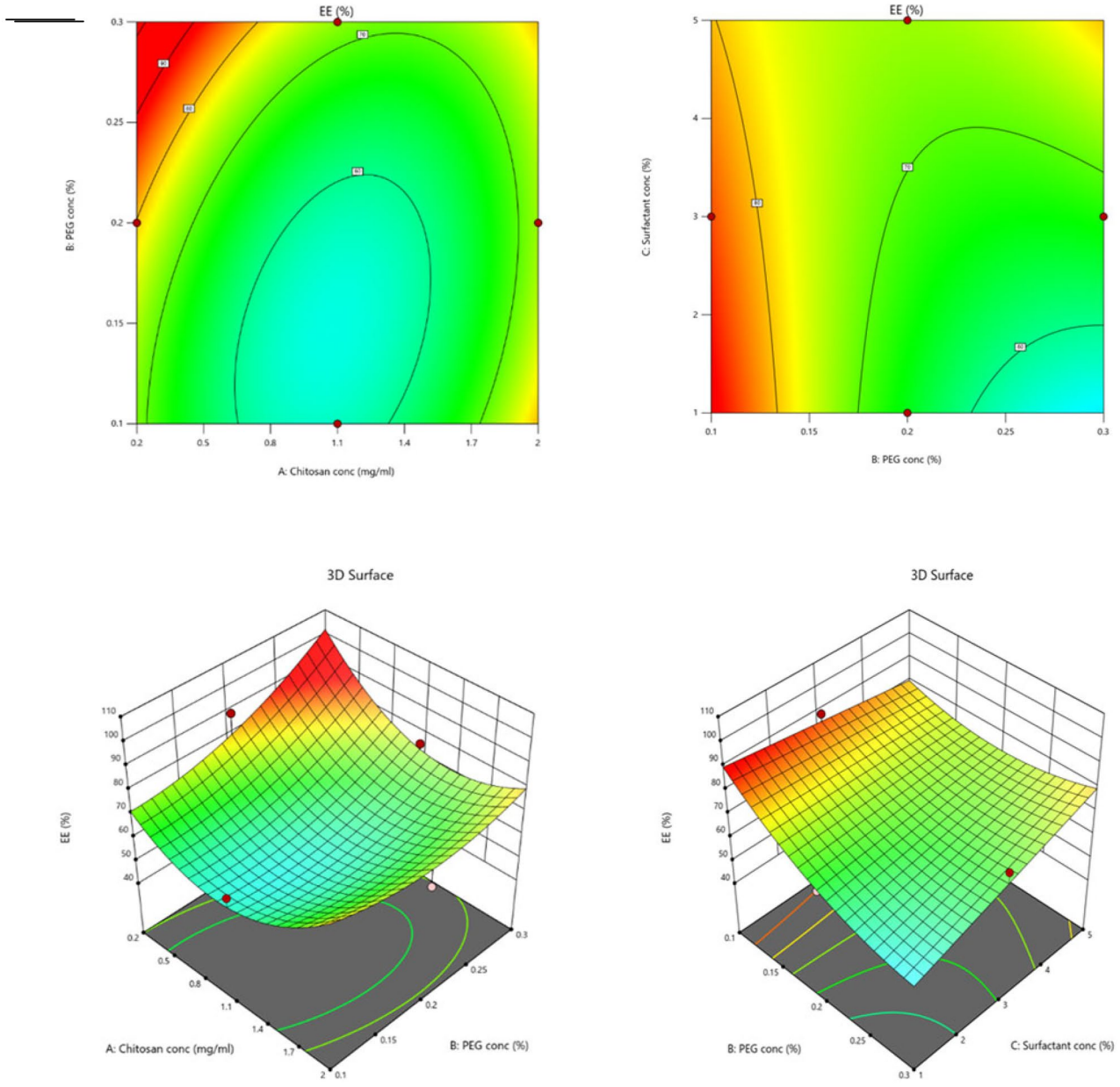

Figure 2. Contour plots (A) and three-dimensional response surface plots (B) for EE (Y_1).

Table 4. Predicted and observed values for encapsulation efficiency of the optimized nanoformulation.

Optimized response	Predicted mean	Predicted median	Observed	Std Dev	95% CI low for mean	95% CI high for mean
EE	95.4291	95.4291	93.87	7.14616	81.5567	109.302

Characterization studies

To determine the physical diversity of crystal formations, XRD investigations were conducted. The XRD pattern of chitosan nanoparticles is seen in Figure 3. The pattern indicates that the chitosan nanoparticle is amorphous since the typical peaks at θ = 20° and 30° exhibit a diminished peak. For the analysis of the particle through the DLS method, the experiment in terms of high encapsulation efficiency was chosen. Table 5 summarizes the process parameters, Z-average diameter, and poly-dispersion index (PDI) value. DLS results indicated a bell-shaped pattern of particle size distribution where most particles range from 100 to 500 nm (Figure 1). From Table 5, the z-average diameter averaged.2 nm. The surface morphology of CS-PEG GONPSs is shown in Figure 4 at different resolutions. CS-PEG GONPSs were shown to have needle-shaped crystals. It did, however, show amorphous, spherical particles of various sizes.

Cell viability assay

The biocompatibility evaluation of CS-PEG GONPs was studied using human Pancreatic cell line (HPNE). The *in vitro* cytotoxic effects on pancreatic cell line during 72 h of incubation showed no significant effect on cell survival (Figure 5). The results indicate that GO and CS-PEG GONPs are biocompatible showing no toxicity effects on non-cancerous pancreatic cell line. The PANC-1 human pancreatic cancer cell line was utilized to study the anticancer effects of GO and CS-PEG GONPs at various doses (Figure 6). There was a dose-dependent decrease in cell

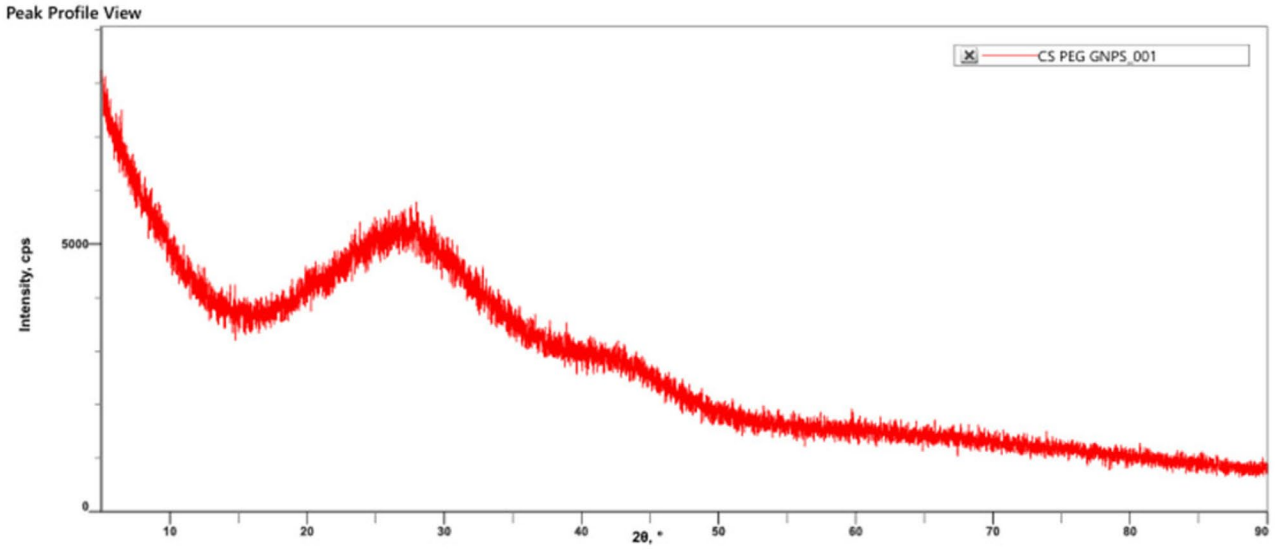

Figure 3. XRD pattern of prepared chitosan nanoparticle.

Table 5. The PDI value and overall Z-average diameter with respect to the highest EE from the experiment.

Chitosan concentration	PEG concentration	Surfactant concentration	Oil loading	Z-average diameter	PDI
0.2 mg/mL	0.28 %	4.85 %	80 µl	265.2	0.524

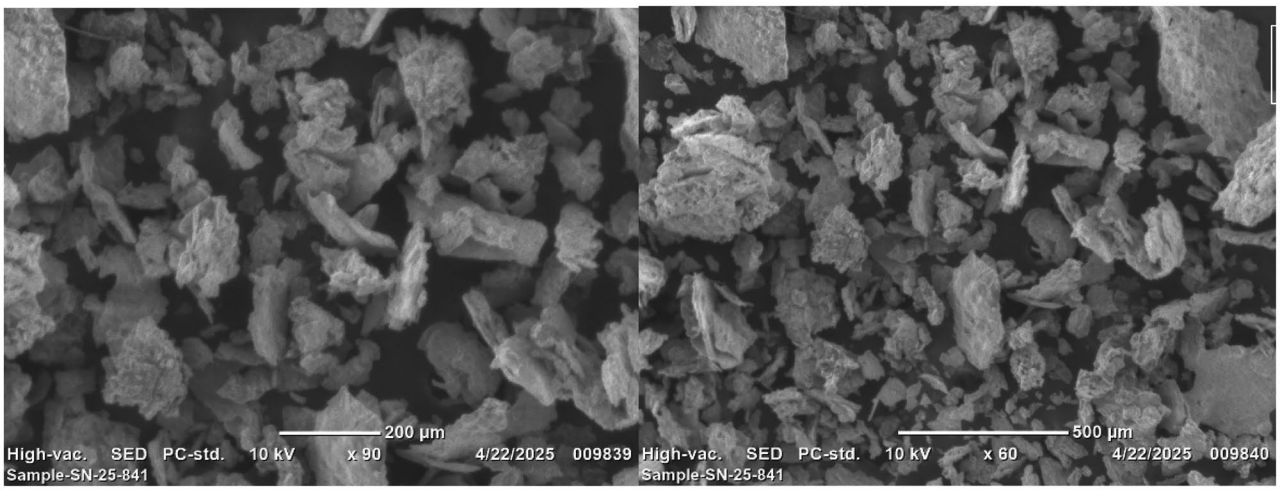

Figure 4. SEM images of CS-PEG GONPSs at ×90 and ×60 resolutions.

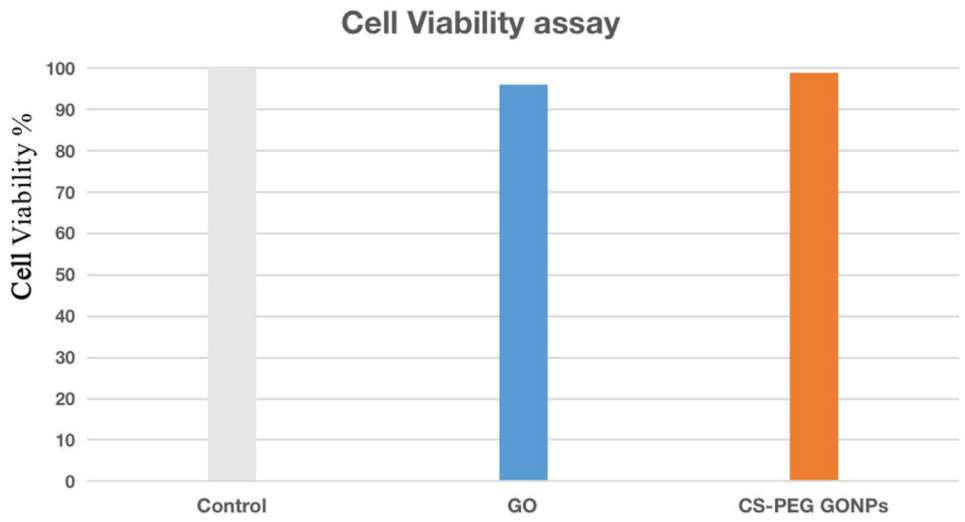

Figure 5. Cell viability assay of GO and CS-PEG GONPs at concentration of 100 µg/ml on Human Pancreatic cell line with untreated HPNE cells as control.

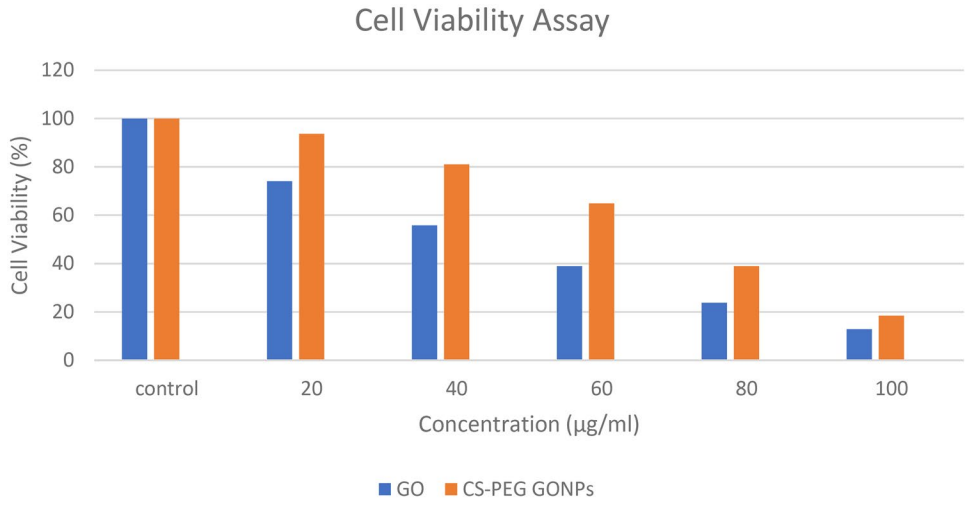

Figure 6. Comparative cell viability assay of GO and CS-PEG GONPs on Human Pancreatic cancer cell line with untreated PANC-1 cell lines as control.

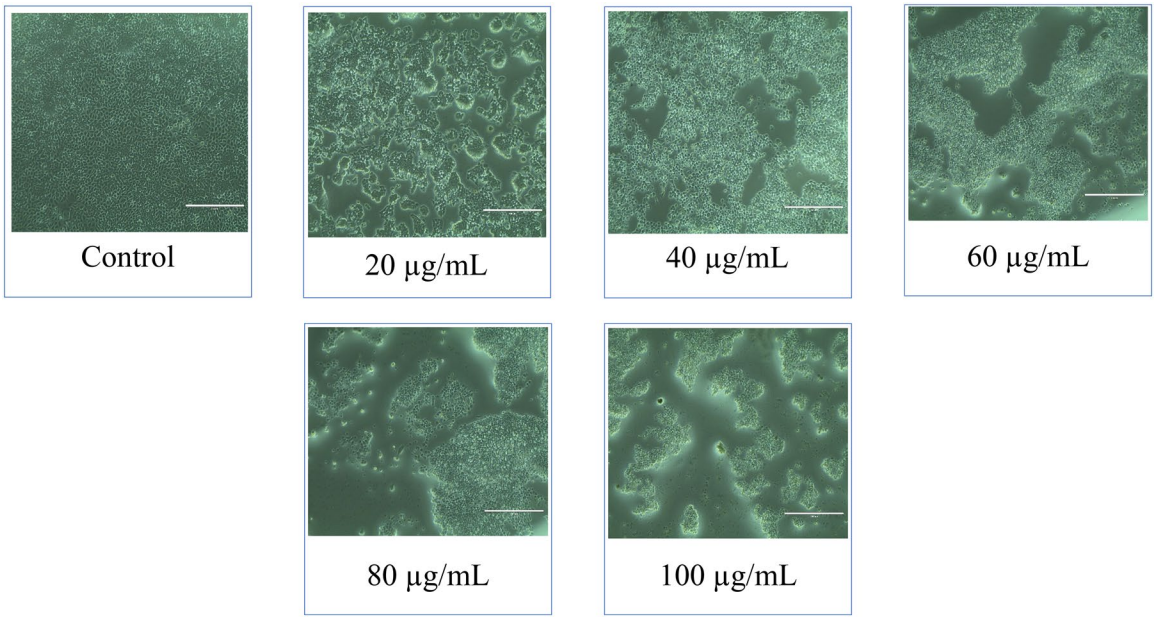

Figure 7. In vitro cytotoxicity analysis of PANC-1 cell line at different concentrations of Geranium oil. The image shows the morphological changes caused by different concentrations of Geranium oil (20 µg/ml to 100 µg/ml) with untreated PANC-1 cells as control.

viability which is indicated. GO lowers cell viability to around 10% at 100 µg/mL. In contrast, CS-PEG GONPs also retains a 20% cell viability at the highest concentration (100 µg/mL). The concentration of GO and CS-PEG GONPs at which 50% cell are viable are about 46.9 µg/mL and 71.49 µg/mL respectively (Figure 6).

Apoptosis fluorescent assay by dual AO/PI staining method

Figures 9 and 10 shows the results of the apoptosis experiment with double AO/PI staining, which again confirmed the anticancer activity of CS-PEG GONPSs and GO. Red fluorescence and a distorted cell shape in the initial phase of apoptosis were clear indications of apoptosis and necrosis in the CS-PEG GONPSs and GO-treated cells.

Discussion

The present study successfully demonstrated the formulation and optimization of CS-PEG GONPs using a Box–Behnken Design (BBD) to maximize encapsulation efficiency (EE) and assess their physicochemical and biological properties. The statistical model showed preferable significance with an R^2 value of 0.8428, confirming the good correlation between experimental and predicted values. As the R^2 value was not greater than 0.95 (which is usually considered as ideal score), the adequacy of the model was further verified by an

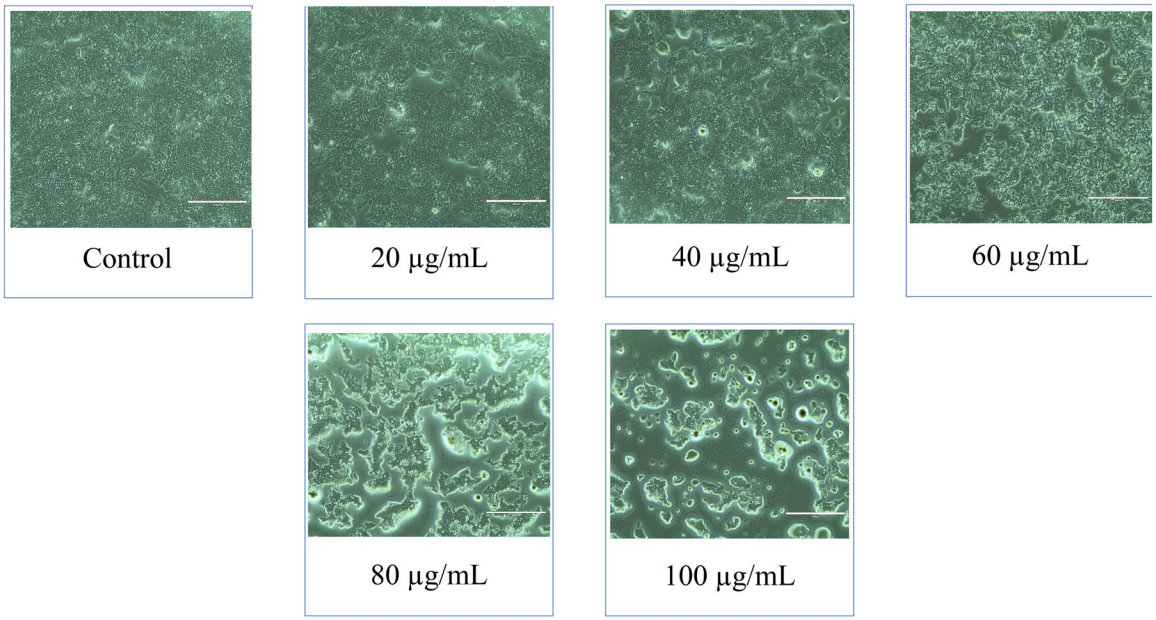

Figure 8. In vitro cytotoxicity analysis of PANC-1 cell line at different concentrations of CS-PEG GONPs. The image shows the morphological changes caused by different concentrations of CS-PEG GONPs (20 µg/ml to 100 µg/ml) with untreated PANC-1 cells as control.

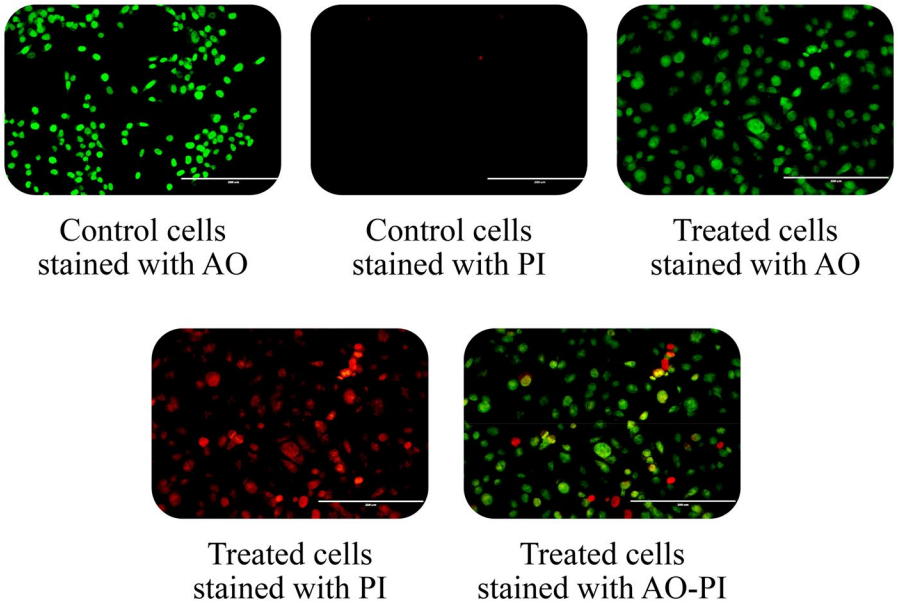

Figure 9. Apoptosis assay by dual AO/PI staining of CS-PEG GONPSs on PANC-1 cell line.

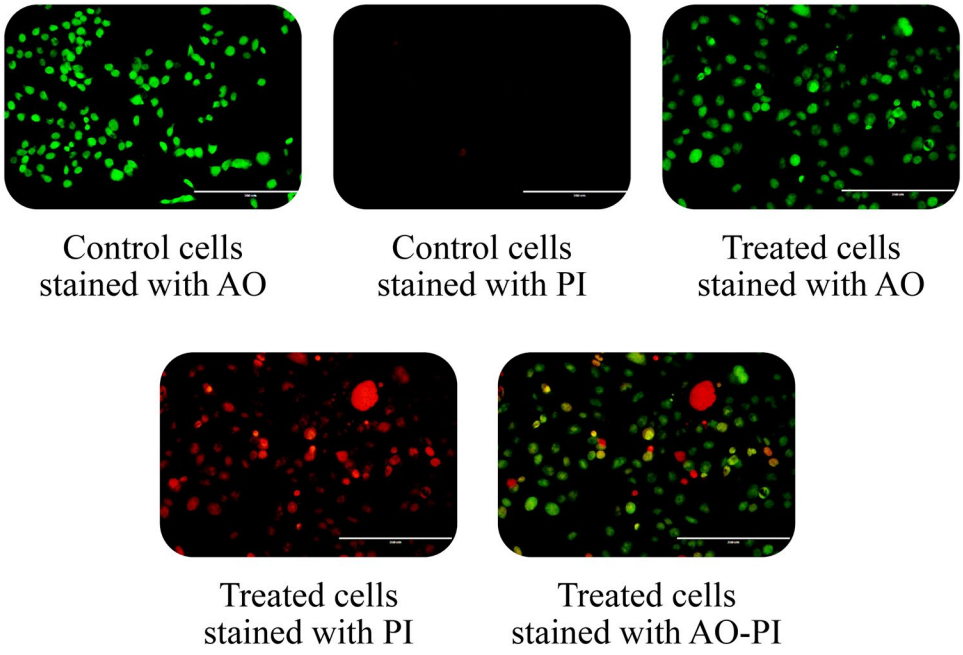

Figure 10. Apoptosis assay by dual AO/PI staining of GO on PANC-1 cell line.

adequate precision ratio of 8.593, signifying an acceptable signal-to-noise ratio and the reliability of the quadratic equation for predicting EE within the experimental design space.

The findings revealed that encapsulation efficiency was significantly influenced by chitosan, PEG, and surfactant concentrations, as indicated by the positive coefficients in the regression model. The synergistic interaction between PEG and surfactant concentration enhanced EE, possibly due to improved emulsification and stabilization of the polymer–oil interface during nanoparticle formation. Similar trends have been observed in polymeric nanoformulations, where PEG acts as a steric stabilizer reducing particle aggregation and improving the dispersion of hydrophobic drug components within the polymeric matrix.[17–19] The quadratic model also identified that increasing chitosan concentration beyond an optimum level led to a decline in EE, which can be attributed to the increased viscosity of the solution, limiting the diffusion of the oil phase and thus reducing encapsulation efficiency.[19]

The optimized formulation parameters −0.2 mg/mL chitosan, 0.28% PEG, and 4.85% surfactant yielded nanoparticles with 93.87% observed EE, which closely matched the predicted value (95.42%). Here, the lower concentration of chitosan and PEG were maintained which had their effect to attain the better encapsulation efficiency. These results confirm that the statistical approach can effectively guide the rational design of nanoparticle formulations by minimizing experimental trials and improving reproducibility.[18]

The characterization studies supported the formation of an amorphous nanostructure, as evidenced by the diminished diffraction peaks in the XRD spectrum. The disappearance of the characteristic crystalline peaks of chitosan upon crosslinking with TPP suggests that ionic interaction between the phosphate groups of TPP and amino groups of chitosan disrupts the crystalline order, resulting in an amorphous, flexible polymer network.[20,21] This amorphous nature enhances drug loading capacity and facilitates a controlled release profile, consistent with previous reports on chitosan-based nanocarriers.[5,22]

Dynamic Light Scattering (DLS) analysis revealed a mean particle size of 265.2 nm with a 0.524 PDI value, indicating less uniform distribution. Even though nanoparticle was synthesized, formation of nanoparticle aggregates moderately increased the particle size and PDI value. Nanoparticles with sizes below 300 nm are known to possess favorable pharmacokinetic properties, enabling cellular uptake and tissue penetration.[22] The moderately narrow size distribution obtained suggests a good emulsification process during nanoparticle formation. Aggregation plays a very crucial role in the drug delivery and it is important to control the formation of aggregates during nanoparticle synthesis process in the future studies. The observed morphology in SEM images—spherical, amorphous particles with minimal agglomeration—further confirmed successful encapsulation and stabilization by PEG. The similarity of morphological and crystalline patterns between our study and that of Zaman et al.[23] reinforces the reproducibility of the polymer–TPP interaction mechanism in nanoparticle synthesis.

The biological evaluation demonstrated distinct cytotoxic behavior between pure geranium oil (GO) and its nanoparticle formulation (CS-PEG GONPs). The marked reduction in cell viability with increasing GO concentration suggests potent anticancer activity, likely due to the high content of monoterpenes and sesquiterpenes known for inducing apoptosis in cancer cells.[24] Although ethanol was used as a transient solvent during formulation, it was removed during nanoparticle preparation, minimizing the likelihood of solvent-induced cytotoxic effects. Modulation of cytotoxicity has been widely reported in nanoparticle-based essential oil delivery systems.[25,26]

At the highest tested concentration (100 µg/ml), the CS-PEG GONPs retained around 20% cell viability,

compared to only 10% for GO, implying that nanoencapsulation attenuates the direct toxic impact of the oil. The polymeric matrix may act as a protective barrier that allows sustained release of the oil components over time, preventing abrupt exposure and toxicity. This behavior aligns with the findings of Kumbhar et al.,[25] who observed a similar protective effect of chitosan nanoparticles encapsulating plant-derived oils on cancer cells. The cytotoxicity evaluation on non-cancerous cells provides the biocompatible nature of polymers used such as chitosan and PEG. Also, the essential oils have shown acceptable safety profiles in previous studies. Cell survival was not affected when the developed nanoencapsulation was administered to cells, thus the nanoformulation can be developed for therapeutic advancements in PDAC treatments.[6,27]

The AO/PI dual staining assay confirmed the induction of apoptosis as the primary mechanism of cytotoxicity for both GO and CS-PEG GONPs. The predominance of orange and red fluorescent cells indicated chromatin condensation and membrane damage typical of apoptotic and necrotic pathways. However, the relatively higher proportion of viable green fluorescent cells in the CS-PEG GONP-treated group compared to GO suggests that nanoparticle formulation may reduce necrotic cell death, promoting a more regulated apoptotic pathway.[7] This could be advantageous in minimizing inflammatory responses in therapeutic applications.[28–30]

Overall, the study confirms that CS-PEG GONPs offer an effective strategy for encapsulating geranium essential oil, providing enhanced stability, controlled release, and reduced cytotoxicity compared to free oil. The combination of chitosan and PEG yielded nanoparticles with excellent physicochemical properties and acceptable particle size for biomedical use[31,32] The BBD optimization approach proved highly efficient in defining the optimal conditions for nanoparticle synthesis with high encapsulation efficiency. In final report, the successful optimization and characterization of CS-PEG GONPs demonstrate their potential as a promising nanocarrier system for the safe and efficient delivery of geranium oil in cancer therapy. Chitosan encapsulation provides increased stability and sustained release characteristics and studies on drug release kinetics within the cancer microenvironment is crucial to better understand the behavior of the nanoparticles. Research on in vivo pharmacokinetics, targeted delivery, and long-term cytotoxicity has to be explored in future to fully evaluate the therapeutic potential of this system.

Conclusion

This study found that ionic gelation was an effective method for producing chitosan nanoparticles with geranium essential oil. Through the application of a three-variable Box-Behnken Design (BBD) within the response surface methodology framework, the research determined the relatively optimal conditions for the production of magnetic stirring-based chitosan/PEG-geranium oil nanoparticles. 0.2 mg/mL of chitosan content, 0.28% PEG content, 4.85% surfactant content, and an oil load of 80 µl were reported to be achieving the acceptable encapsulation efficiency (EE%) value of 93.87%. The characterization of the resulting nanoparticles using X-ray diffraction (XRD), Dynamic Light Scattering (DLS), and Scanning Electron Microscopy (SEM) was conducted to determine their crystallinity (amorphous), size (<250 nm), and morphological characteristics which should be studied further to improve the nondispersive characteristic of the nanoparticle for the application of drug delivery. The comparative cell line (PANC-1) studies were done between GO and CS-PEG GONPSs, and the anticancer activity was observed by conducting a Cytotoxicity assay and an Apoptosis Fluorescent dual AO/PI staining method, which showed a dose-dependent activity and also the balanced cytotoxicity of CS-PEG GONPSs at 100 µg/ml in order to minimize the damage of normal cells during application of the drug. Through this integrated approach, combining targeted delivery with comprehensive physicochemical characterization, the study aims to develop a promising therapeutic platform contributing to more effective treatment strategies for PDAC and further validation through *in vivo* studies and comprehensive safety evaluations is required before considering therapeutic applications.

Acknowledgments

The authors are thankful to the authority of Vels Institute of Science, Technology and Advanced Studies (VISTAS), Saveetha Dental College & Hospitals, Saveetha Institute of Medical and Technical Sciences (SIMATS), Saveetha University, Chennai, and Tamil Nadu for providing the necessary facilities and support.

Author contributions

CRediT: **Manjunathan Jagadeesan**: Resources, Software; **Pasiyappazham Ramasamy**: Project administration, Supervision, Writing – review & editing; **Ambiga Somasundaram**: Data curation, Software; **Chandramohan Govindasamy**: Formal analysis, Funding acquisition; **Khalid M. Almutairi**: Funding acquisition, Resources; **Krishna Prakash Arunachalam**: Resources, Software; **Meenambiga Setti Sudharsan**: Conceptualization, Formal analysis.

Disclosure statement

The authors declare no competing financial interests or personal relationships that could influence the work reported in this study.

Funding

The authors express their sincere appreciation to the Ongoing Research Funding Program, (ORF-2025-712), King Saud University, Riyadh, Saudi Arabia.

Data availability statement

Data will be available on request.

References

[1] Bray, F.; Ferlay, J.; Soerjomataram, I.; Siegel, R. L.; Torre, L. A.; Jemal, A. Global Cancer Statistics 2018: GLOBOCAN Estimates

of Incidence and Mortality Worldwide for 36 Cancers in 185 Countries. *CA. Cancer J. Clin.* **2018**, *68*, 394–424. DOI: 10.3322/caac.21492.

[2] Sung, H.; Ferlay, J.; Siegel, R. L.; Laversanne, M.; Soerjomataram, I.; Jemal, A.; Bray, F. Global Cancer Statistics 2020: GLOBOCAN Estimates of Incidence and Mortality Worldwide for 36 Cancers in 185 Countries. *CA. Cancer J. Clin.* **2021**, *71*, 209–249. DOI: 10.3322/caac.21660.

[3] Mahadevan, K. K.; McAndrews, K. M.; LeBleu, V. S.; Yang, S.; Lyu, H.; Li, B.; Sockwell, A. M.; Kirtley, M. L.; Morse, S. J.; Moreno Diaz, B. A.; et al. KRASG12D Inhibition Reprograms the Microenvironment of Early and Advanced Pancreatic Cancer to Promote FAS-Mediated Killing by CD8+ T Cells. *Cancer Cell.* **2023**, *41*, 1606–1620.e8. DOI: 10.1016/j.ccell.2023.07.002.

[4] Ischenko, I.; D'Amico, S.; Rao, M.; Li, J.; Hayman, M. J.; Powers, S.; Petrenko, O.; Reich, N. C. KRAS Drives Immune Evasion in a Genetic Model of Pancreatic Cancer. *Nat. Commun.* **2021**, *12*, 1482. DOI: 10.1038/s41467-021-21736-w.

[5] Nguyen, G. H.; Le, X. T. Palmarosa Essential Oil Encapsulated in Chitosan Nanoparticles by Ionotropic Gelation: Formulation and Characterization. *IOP Conf. Ser. Earth Environ. Sci.* **2021**, *947*, 012002. DOI: 10.1088/1755-1315/947/1/012002.

[6] Bal, K.; Küçükertuğrul Çelik, S.; Şentürk, S.; Kaplan, Ö.; Eker, E. B.; Gök, M. K. Recent Progress in Chitosan-Based Nanoparticles for Drug Delivery: A Review on Modifications and Therapeutic Potential. *J. Drug Target.* **2025**, *33*, 1366–1393. DOI: 10.1080/1061186X.2025.2502956.

[7] Edalatian Tavakoli, S.; Motavalizadehkakhky, A.; Homayouni Tabrizi, M.; Mehrzad, J.; Zhiani, R. Study of the Anti-Cancer Activity of a Mesoporous Silica Nanoparticle Surface Coated with Polydopamine Loaded with Umbelliprenin. *Sci. Rep.* **2024**, *14*, 11450. DOI: 10.1038/s41598-024-62409-0.

[8] Babaei, M.; Kashanian, S.; Salemi, Z. Optimization of the Redox-Sensitive Doxorubicin Loaded Chitosan-Based Nanoparticles by Box–Behnken Experimental Design; **2024**. DOI: 10.21203/rs.3.rs-3828026/v1.

[9] Yousefi, M.; Khanniri, E.; Sohrabvandi, S.; Khorshidian, N.; Mortazavian, A. M. Encapsulation of Heracleum Persicum Essential Oil in Chitosan Nanoparticles and Its Application in Yogurt. *Front. Nutr.* **2023**, *10*, 1130425. DOI: 10.3389/fnut.2023.1130425.

[10] Melo, M. N.; Pereira, F. M.; Rocha, M. A.; Ribeiro, J. G.; Junges, A.; Monteiro, W. F.; Diz, F. M.; Ligabue, R. A.; Morrone, F. B.; Severino, P.; et al. Chitosan and Chitosan/PEG Nanoparticles Loaded with Indole-3-Carbinol: Characterization, Computational Study and Potential Effect on Human Bladder Cancer Cells. *Mater. Sci. Eng. C Mater. Biol. Appl.* **2021**, *124*, 112089. DOI: 10.1016/j.msec.2021.112089.

[11] Roshan, Z.; Haddadi-Asl, V.; Ahmadi, H.; Moussaei, M. Curcumin-Encapsulated Poly(Lactic- *Co* -Glycolic Acid) Nanoparticles: A Comparison of Drug Release Kinetics from Particles Prepared via Electrospray and Nanoprecipitation. *Macro. Mater. Eng.* **2024**, *309*, 2400040. DOI: 10.1002/mame.202400040.

[12] Werdin González, J. O.; Jesser, E. N.; Yeguerman, C. A.; Ferrero, A. A.; Fernández Band, B. Polymer Nanoparticles Containing Essential Oils: New Options for Mosquito Control. *Environ. Sci. Pollut. Res. Int.* **2017**, *24*, 17006–17015. DOI: 10.1007/s11356-017-9327-4.

[13] Mohamed, J. M. M.; Ahmad, F.; El-Sherbiny, M.; Al Mohaini, M. A.; Venkatesan, K.; Alrashdi, Y. B. A.; Eldesoqui, M. B.; Ibrahim, A. E.; Dawood, A. F.; Ibrahim, A. M.; et al. Optimization and Characterization of Quercetin-Loaded Solid Lipid Nanoparticles for Biomedical Application in Colorectal Cancer. *Cancer Nano.* **2024**, *15*, 16. DOI: 10.1186/s12645-024-00249-3.

[14] Fahmy, S. A.; Ramzy, A.; Mandour, A. A.; Nasr, S.; Abdelnaser, A.; Bakowsky, U.; Azzazy, H. M. E.-S. PEGylated Chitosan Nanoparticles Encapsulating Ascorbic Acid and Oxaliplatin Exhibit Dramatic Apoptotic Effects against Breast Cancer Cells. *Pharmaceutics.* **2022**, *14*, 407. DOI: 10.3390/pharmaceutics14020407.

[15] Jaisankar, E.; Azarudeen, R. S.; Thirumarimurugan, M. A Study on the Effect of Nanoscale MgO and Hydrogen Bonding in Nanofiber Mats for the Controlled Drug Release along with *In Vitro* Breast Cancer Cell Line and Antimicrobial Studies. *ACS Appl. Bio Mater.* **2022**, *5*, 4327–4341. DOI: 10.1021/acsabm.2c00519.

[16] Priya M, S. V. In Vitro Evaluation of Apoptotic Effects of Different Viruddha Samyogas of Kshira in Human Hepatic WRL-68 Cell Line. *AJBR.* **2024**, *27*, 315–319. DOI: 10.53555/AJBR.v27i3.1362.

[17] Raghavendra Naveen, N.; Kurakula, M.; Gowthami, B. Process Optimization by Response Surface Methodology for Preparation and Evaluation of Methotrexate Loaded Chitosan Nanoparticles. *Mater. Today Proc.* **2020**, *33*, 2716–2724. DOI: 10.1016/j.matpr.2020.01.491.

[18] Tahir, I.; Millevania, J.; Wijaya, K.; Wahab, R. A.; Kurniawati, W.; Mudasir. Optimization of Thiamine Chitosan Nanoemulsion Production Using Sonication Treatment. *Res. Eng.* **2023**, *17*, 100919. DOI: 10.1016/j.rineng.2023.100919.

[19] Parseghian, L.; Behboudi, H.; Ebrahimi, S. N.; Rafati, H. Antiproliferative Activity of Prepared Aloe Vera Leaf Skin Extract-Loaded Essential Oil Nanoemulsions Using Box-Behnken Design. *Ind. Crops Prod.* **2025**, *228*, 120928. DOI: 10.1016/j.indcrop.2025.120928.

[20] Ali, M. E. A.; Aboelfadl, M. M. S.; Selim, A. M.; Khalil, H. F.; Elkady, G. M. Chitosan Nanoparticles Extracted from Shrimp Shells, Application for Removal of Fe(II) and Mn(II) from Aqueous Phases. *Sep. Sci. Technol.* **2018**, *53*, 2870–2881. DOI: 10.1080/01496395.2018.1489845.

[21] Ahmed, M. E.; Mohamed, M. I.; Ahmed, H. Y.; Elaasser, M. M.; Kandile, N. G. Fabrication and Characterization of Unique Sustain Modified Chitosan Nanoparticles for Biomedical Applications. *Sci. Rep.* **2024**, *14*, 13869. DOI: 10.1038/s41598-024-64017-4.

[22] Almeida, K. B.; Araujo, J. L.; Cavalcanti, J. F.; Romanos, M. T. V.; Mourão, S. C.; Amaral, A. C. F.; Falcão, D. Q. In Vitro Release and Anti-Herpetic Activity of Cymbopogon Citratus Volatile Oil-Loaded Nanogel. *Revista Brasileira de Farmacognosia.* **2018**, *28*, 495–502. DOI: 10.1016/j.bjp.2018.05.007.

[23] Zaman, M.; Butt, M. H.; Siddique, W.; Iqbal, M. O.; Nisar, N.; Mumtaz, A.; Nazeer, H. Y.; Alshammari, A.; Riaz, M. S. Fabrication of PEGylated Chitosan Nanoparticles Containing *Tenofovir alafenamide*: Synthesis and Characterization. *Molecules.* **2022**, *27*, 8401. DOI: 10.3390/molecules27238401.

[24] Neumann, M.; Prahl, S.; Caputi, L.; Hill, L.; Kular, B.; Walter, A.; Patallo, E. P.; Milbredt, D.; Aires, A.; Schöpe, M.; et al. Hairy Root Transformation of Brassica Rapa with Bacterial Halogenase Genes and Regeneration to Adult Plants to Modify Production of Indolic Compounds. *Phytochemistry.* **2020**, *175*, 112371. DOI: 10.1016/j.phytochem.2020.112371.

[25] Kumbhar, S. T.; Patil, R. Y.; Bhatia, M. S.; Choudhari, P. B.; Gaikwad, V. L. Synthesis and Characterization of Chitosan Nanoparticles Decorated with Folate and Loaded with Dasatinib for Targeting Folate Receptors in Cancer Cells. *OpenNano.* **2022**, *7*, 100043. DOI: 10.1016/j.onano.2022.100043.

[26] Karimivaselabadi, A.; Osanloo, M.; Ghanbariasad, A.; Zarenezhad, E.; Hosseini, H. Comparison of Chitosan Nanoparticles Containing Lippia Citriodora Essential Oil and Citral on the Induction of Apoptosis in A375 Melanoma Cells. *BMC Complement. Med. Ther.* **2023**, *23*, 435. DOI: 10.1186/s12906-023-04268-2.

[27] Burke, Y. D.; Stark, M. J.; Roach, S. L.; Sen, S. E.; Crowell, P. L. Inhibition of Pancreatic Cancer Growth by the Dietary Isoprenoids Farnesol and Geraniol. *Lipids.* **1997**, *32*, 151–156. DOI: 10.1007/s11745-997-0019-y.

[28] Han, Z.; Gao, M.; Wang, Z.; Peng, L.; Zhao, Y.; Sun, L. pH/NIR-Responsive Nanocarriers Based on Mesoporous Polydopamine Encapsulated Gold Nanorods for Drug Delivery and

Thermo-Chemotherapy. *J. Drug Deliv. Sci. Technol.* **2022**, *75*, 103610. DOI: 10.1016/j.jddst.2022.103610.

[29] Ma, Z.; Han, Z.; Wan, M.; Wang, Z.; Gao, M.; Zhao, Y.; Sun, L. Development of a pH/NIR/Temperature-Responsive Drug Delivery System Using AuNRs@ZnO@mPDA Nanoparticles for Synergistic Cancer Therapy. *Surf. Interf.* **2025**, *61*, 106153. DOI: 10.1016/j.surfin.2025.106153.

[30] Gao, M.; Han, Z.; Zhang, X.; Zou, X.; Peng, L.; Zhao, Y.; Sun, L. Construction of Double-Shelled Hollow Ag_2S@Polydopamine Nanocomposites for Fluorescence-Guided, Dual Stimuli-Responsive Drug Delivery and Photothermal Therapy. *Nanomaterials (Basel).* **2022**, *12*, 2068. DOI: 10.3390/nano12122068.

[31] Sorasitthiyanukarn, F. N.; Muangnoi, C.; Thaweesest, W.; Ratnatilaka Na Bhuket, P.; Jantaratana, P.; Rojsitthisak, P.; Rojsitthisak, P. Polyethylene Glycol-Chitosan Oligosaccharide-Coated Superparamagnetic Iron Oxide Nanoparticles: A Novel Drug Delivery System for Curcumin Diglutaric Acid. *Biomolecules.* **2020**, *10*, 73. DOI: 10.3390/biom10010073.

[32] Tığlı Aydın, R. S.; Pulat, M. 5-Fluorouracil Encapsulated Chitosan Nanoparticles for PH-Stimulated Drug Delivery: Evaluation of Controlled Release Kinetics. *J. Nanomater.* **2012**, *2012*, 1–10. DOI: 10.1155/2012/313961.